academicJournals

Journal of Geology and Mining Research

Full Length Research Paper

New approaches to monitoring, analyzing and predicting slope instabilities

Upasna Chandarana Kothari* and Moe Momayez

Mining and Geological Engineering, University of Arizona, Arizona, USA.

In a mining operation, any noticeable instability can pose a catastrophic threat to the lives of workers. Slope instability can also disrupt the chain of production in a mine, resulting in a loss to the business. Due to the potential threat associated with rock mass movement, it is necessary to be able to predict the time of slope failure. In the past couple of decades, innovations in slope monitoring equipment have made it possible to scan a broad rock face in a short period of time with sub-millimeter accuracy. The data collected from instruments such as Slope Stability Radar (SSR) are commonly used for slope failure predictions, however, it has been challenging to find a method that can provide the time of failure accurately. The aim of this paper is to demonstrate the use of different methods to optimize slope failure predictions. Various methods investigated for research presented in this article include: Minimum Inverse Velocity (MIV), Maximum Velocity (MV), Log Velocity (LV), Log Inverse Velocity (LIV), and Spline regression (SR). Based on the different methods investigated, the Minimum Inverse Velocity method provided the most consistent and accurate results. The use of MIV method resulted in about 75% better predictions than the other methods.

Key words: Monitoring, slope failure, slope instabilities, slope movement, rock failure.

INTRODUCTION

Monitoring slope instability and rock mass movements is a basic and prevalent practice in the field of geomechanics. In a mining environment, any noticeable instability could pose a potential threat to the lives of employees as well as the business. Most rock slope failures are associated with creep deformation and the causes of instability are often complex. It is, therefore, challenging to predict slope failure time accurately. However, with the capability and availability of the modern slope monitoring technology, it is now possible to scan large moving slopes in a matter of minutes with a sub-millimeter accuracy. Consequently, operators are better prepared to face the consequences of slope failures in open pit mines (Osasan and Stacey, 2014). Along with slope monitoring, early warning systems (EWS) help prepare for large slope failures. EWSs can be considered as a cost effective alternative that help reduce risks or help prepare for risks associated with large moving slopes that cannot be mitigated (Intrieri et al., 2012). EWSs are built into monitioring modern

*Corresponding author. E-mail: upasnap@gmail.com.

technology that alarm the users of any moving areas. The system can be set up to warn the user of any movement that seems to be higher than a set threshold based on the history and geological factors associated with the area.

Over the years, many attempts have been made to develop a method to predict the time of failure. The challenge in predicting slope failure stems from the fact that factors influencing instability such as ground conditions, physical and geomorphological processes, along with human activities are either not known completely or difficult to determine continuously (Nie et al., 2016). Therefore, instead of developing a phenomenological model of slope failure, practitioners have relied on a detailed analysis of slope deformation (Chen et al., 2015). Calculating the factor of safety (FOS) of pit walls is crucial while designing mine slope walls and performing per failure slope analysis. Most mines require having a FOS of 1.0 or higher, whereas an FOS below 1.0 is considered as unsafe work environment. A study was performed at Çöllolar mine in Elbistan that shows how important FOS is (Ozbay and Cabalar, 2014). There were two landslides at the Çöllolar mine within 4 days; one of the landslides was caused due to the high groundwater levels as well as an inappropriate FOS. The study concluded that the first landslide caused the second landslide (Ozbay and Cabalar, 2014).

Deformation data collected by various instruments is the most important piece of information needed to perform time series analysis for slope failure predictions (Liu et al., 2014; Mazzanti et al., 2015). Both time and deformation data are readily available from the monitoring equipment used for geotechnical risk management analysis. Some of the traditional and more advanced technologies include but are not limited to survey network, tension crack mapping, wireline extensometers, ground-based real aperture radar, synthetic aperture radar, and satellite-based synthetic aperture radar (Chandarana et al., 2016).

In the past decade, there has been an increased use of ground-based radars, both real and synthetic aperture. Coupled with simple and cost-effective technologies such as wireline extensometers, prisms and tension crack mapping enhance active slope monitoring. The top three advantages of ground-based radars as stated by Dick et al. (2015) include: (i) broad area coverage, (ii) near real-time slope movement data, and (iii) no additional equipment installation is needed, reducing the risk of workers being exposed to rock fall hazard. As the radar technology becomes prevalent in the mining industry for monitoring slope movements, it is essential to understand the basics of its use. The ground-based radars provide a Line-Of-Sight (LOS) data set that is used to monitor slopes as well as make necessary slope failure predictions (Harries et al., 2006). Usually, the data sets provided by the monitoring systems are large; it is important to narrow down to the time window that

demonstrates any accelerating trends to make failure predictions. Accelerating trends in deformation are an indicator of possible unstable slopes leading to slope failures. It is also crucial to reduce the size of the data being used by only focusing on consecutive and neighboring pixels that demonstrate movement instead of a large cluster of pixels. Using a large area of the slope will produce misleading failure predictions times or show that the slopes are steady, as a larger data set will average the moving and nonmoving pixels together. It is a common practice to select a single pixel or a small cluster of pixels for analysis instead of utilizing the whole data set provided by the radar systems (Dick et al., 2015). While choosing the correct area for slope failure analysis, it is important to remember that the true magnitude of the deformation data is based on the LOS between the radar and the area being monitored. If the area of interest is not in the direct LOS, the amount of deformation being measured will be smaller than the real deformation (Carlá et al., 2017a). With this downside in the data acquired from monitoring systems, there will always be some room for error of a failure time prediction. There are many examples of the use of monitoring data demonstrated by different authors (Cahill and Lee, 2006; Carlá et al., 2017b; Crosta and Agliardi, 2003; Day and Seery, 2007; Federico et al., 2012; Harries and Roberts, 2007; Little, 2006; Ramsden et al., 2015; Rose and Hungr, 2006).

The most common form of data acquired from monitoring systems consists of time and deformation/displacement data. Monitoring systems will typically record an increase in deformation data until the slope collapses or until the slope movement is too fast for the monitoring system to capture (Chandarana et al., 2016). The time and deformation data will help identify if the slope movement resembles progressive, steady or regressive deformation (Figure 1). Zavodni and Broadbent (1978) used the empirical data from several open pit mines to identify the difference between progressive and regressive slope movement (1978). The terms progressive and regressive displacement can cause confusion, hence the alternative names are unstable and stable displacement, respectively. Progressive displacement is seen when a slope starts to deform at a slow rate and then start to accelerate till the point of collapse. Steady displacement is what the name suggests, when a slope deforms at a constant rate it is known as steady displacement. A slope with decelerating movement is referred to as regressive displacement; this type of movement usually does not cause any failures. If a regressive movement results in a failure, it is usually a response to some mining activity (Call et al., 2000).

Predicting slope failure time has become a common practice at all active mining sites. If the observed slope movement is deemed to cause an imminent collapse, it becomes critical to be able to predict a conservative time of the failure. In order to make a prediction that allows
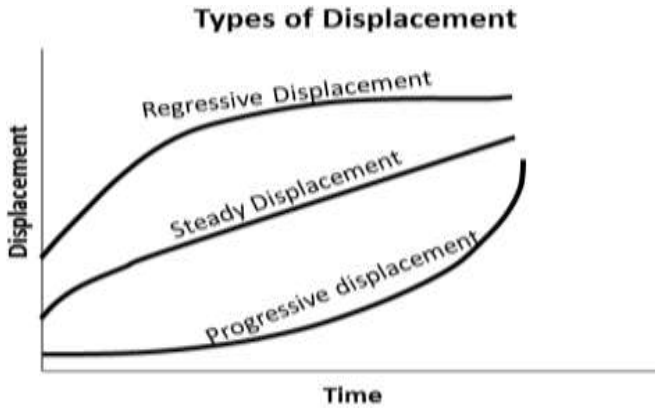
Types of Displacement

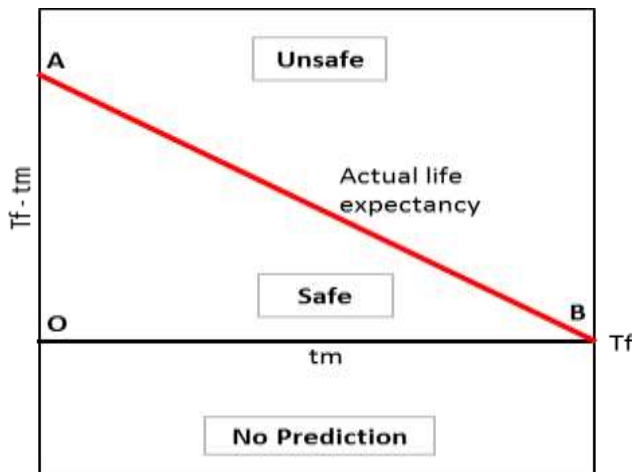**Figure 1.** Progressive, steady, and regressive displacement.

Figure 2. Distinction between safe and unsafe failure prediction.

ample evacuation time, the forecast should allow for a time before the actual slope failure. If the projected time of failure is earlier than the real time of failure, it is referred to as a safe prediction. Figure 2 displays a visual diagram of safe and unsafe prediction. The line AB represents the life expectancy of the moving slope. At point B, Tf represents the time of the collapse. If the slope failure prediction is made at a time below the line AB, it will be recognized as a safe prediction, and if the time estimate falls in the area above the line AB, it is regarded an unsafe prediction. In Figure 2, the x-axis represents the time at any instance of failure prediction, and the y-axis represents predicted life expectancy at tm, using Tf - tm. A safe prediction allows for evacuation or emergency preparedness before the actual event (Mufundirwa et al., 2010). If the prediction is in the unsafe zone, it physically means that the failure will occur prior to the predicted time giving limited or no time to anyone working in the hazardous area to evacuate (Mufundirwa et al., 2010).

In the past, many attempts have been made to develop a reliable method for predicting the time of slope failure.

Most of these studies have used the inverse velocity method. Another method that has gained popularity in the past decade is the Fuzzy Neural Network Approach. The failure prediction methods are briefly discussed below. This paper investigates different methods of predicting the time of slope failure based on historical data. Along with the various methods tried, another important goal of this study is to make a time prediction that falls in the safe zone as identified above. All the data used for the analysis have been obtained from mines with an active ground-based radar program.

## MATERIALS AND METHODS

Current analysis approaches

When a geomechanical failure will occur at an active mine site is the critical question for the geotechnical group that focuses on the slope stability monitoring (Mufundirwa et al., 2010). It is important to get an approximate time of failure at active mines mainly as it will help avoid human loss, reduce damages to property and provide sufficient time to take necessary countermeasures (Federico et al., 2012). It is important to understand the structural geology of the area, climate, groundwater, *in situ* stress conditions, rock mass strengths and seismicity to assess rock failure mechanism (Rose and Hungr, 2006). Monitoring is used at all active mining sites to watch for fast moving slope mass or possible accelerating rock mass movement. Despite the availability of technologies such as global positioning systems (GPS), slope stability radars (SSR), prisms, extensometers and many more, for monitoring slope stability, there is always an uncertainty as to when an actively moving area might collapse (Chandarana et al., 2016). Due to this uncertainty, it is important to have a method that can help predict the time of failure based on the rate of movement to achieve safe and manageable slopes, as well as preventing catastrophes. Catastrophic accidents caused by slope failures have become more manageable with the advent of modern monitoring equipment that have the capability to scan a large slope face within minutes and detect sub-millimeter displacement (Ossan and Stacey, 2014). Described below are the two widely used methods for predicting the time of failure based on deformation data from the modern monitoring systems.

Inverse velocity method (IV)

In 1985, Fukuzono developed the concept of inverse-velocity for predicting the time of slope failure with the help of tests performed in a well-instrumented laboratory while inducing a landslide in soil like material under the influence of water seepage (Fukuzono, 1985). IV method requires the measurement of deformation over time. When a significant acceleration is detected in the deformation rate, an inverse velocity versus time graph is used to make a failure time prediction. A trend line of the inverse velocity is projected to intersect with the time axis. The point at which the trend line crosses the x-axis is the failure time prediction. Fukuzono fitted three types of trend lines, namely: concave, convex and linear curves to the data accumulated from the laboratory tests (Fukuzono, 1985). Based on many tests Fukuzono concluded that the linear trend line gave the best estimate of the failure prediction time (Fukuzono, 1985). The four simple steps below describe IV method:
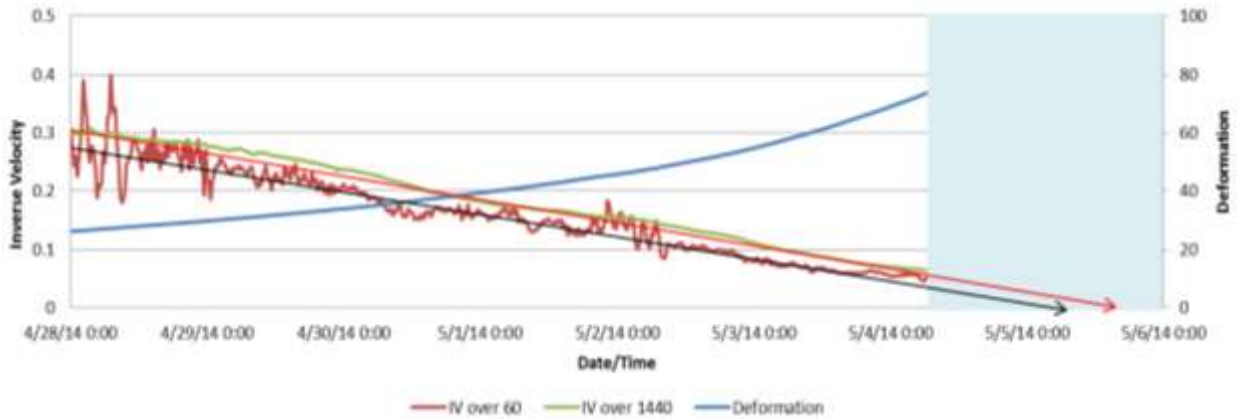
Figure 3. Deformation and inverse velocity of a moving area 24 h before a failure. The blue line represents deformation, red line represents inverse-velocity averaged over 60-min, and green line represents inverse-velocity averaged over 1440 min.
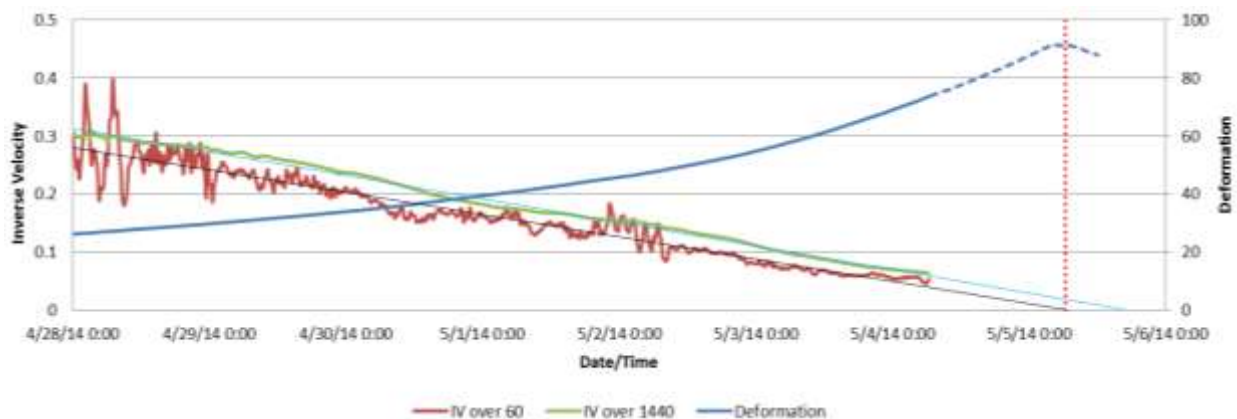
Figure 4. Deformation and inverse velocity of a moving area 24 h before a failure. The blue line represents deformation, red line represents inverse-velocity averaged over 60-min, and green line represents inverse-velocity averaged over 1440 min. Black and blue lines represent the extended best fit lines of the data to help predict the time of failure. The red dotted line represents actual time of failure.

1) Use the deformation and time data to calculate the inverse rate of displacement.
2) Perform a simple linear regression of the inverse rate of displacement. The simple equation $y = mx + b$ is used.
3) Fit a regression line through the inverse velocity versus time data.
4) Extend the best fit line to intersect the time axis to get the time of slope failure prediction.

The most common form of data that radars can produce is deformation and time. Based on the deformation and time data, acceleration, velocity, and inverse velocity can be easily calculated. Often, the radar software readily provides the inverse velocity to use for the analysis. The inverse velocity and deformation data can be plotted together, once a significant rock mass movement is observed (Figure 3). Linear regression and determination of the best fit line in the inverse velocity curve are the next steps in predicting the time of failure. The visual illustration (Figure 3) shows a graph with visible acceleration in the deformation curve. In the example below the graph is based on an actual rock mass failure. The data is a representation of the data collected in a 24-h period before the actual failure time. The best fit line for the averaged inverse velocity is extended to intersect the time-axis (Figure 4). The point at which the inverse velocities intersect the x-axis is the predicted time of slope failure. In the demonstration below, two inverse velocities have been used: one uses an averaging of 1-h time intervals and the other uses averaging of the 24-h time interval. Data smoothing is done to reduce the noise in the data caused by weather or any unintended human interaction. It is easy to make slope failure predictions with data that clearly demonstrates a progressive trend. Slope failure predictions are hard if there is an unclear trend or a trend that lasts for a very short period (Osasan and Stacey, 2014).

Fuzzy neural network

Geology and environmental conditions that occur naturally cannot be assigned a numerical value to solve slope stability problems as this uncertainty keeps slope stability as a fascinating subject for research (Chandarana et al., 2016). The fuzzy set theory has been gaining interest for the past couple of decades, especially in civil
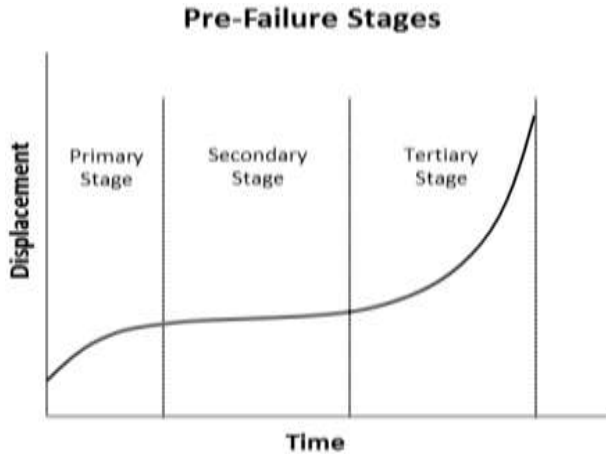
Pre-Failure Stages

Figure 5. Primary stages of pre-failure evolution.

engineering and has been slowly adapted for slope stability research. Many successful types of research have been performed for slope stability analysis using the fuzzy neural network (Hwang et al., 2009; Lin et al., 2009; Ni et al., 1996; Sakellariou and Frentinou, 2005; Wang et al., 2005). Besides these, there are many more studies that use the neural networks to assess slope instability. The studies show that this method helps with the preparedness for a potential slope failure, but this approach cannot be used to predict the time of slope failure.

Zadeh introduced the fuzzy set theory as a class of objectives with a continuum of grades of membership (Zadeh, 1965). In the fuzzy set theory, a set is categorized by a membership function that assigns each object in the set; a grade ranging between zero and one. In machine learning, the fuzzy set theory or neural network is a system adopted from the biological neural network, a system that uses a large number of inputs to solve and estimate different functions. The artificial neural networks are a simplified version of the biological version, but it retains a good structure to provide information on how the neural networks might work (Sakellariou and Frentinou, 2005). In 1992, the fuzzy sets were adopted by Juang et al. for mapping the potential of slope failure (Juang et al., 1992). The primary function of a neural network is to gain experience and accumulate knowledge from the unknown inputs; due to this ability, the artificial neural networks are sometimes used to evaluate the failure potential of moving slopes (Juang et al., 1992).

The basis of the neural network approach is the function of a neuron. A neuron is a unit with the ability to perform a function based on an input X to produce an output Y. Defined below is the relationship between X and Y (Juang et al., 1992):

$$Y_i = f(net_i) \tag{1}$$

$$net_i = \sum_j (W_{ji} X_j - \theta_i) \tag{2}$$

where: net_i = weighted input from all ith neurons. Y_i = output value of ith neuron. W_{ji} = Weight of input data (X_j) from the jth neuron. X_j = input value of the jth neuron. θ_i = weighted biases of the ith neuron. f = transfer or activation function.

A conventional neural network includes three layers: input, output and a hidden layer. Neural networks are categorized into two forms: supervised or unsupervised. A supervised neural network is trained to produce desired outputs based on a set of inputs, whereas an unsupervised network is created by letting the network adjust to

new input data (Sakellariou and Frentinou, 2005). Juang et al. demonstrated a successful use of neural network based on the model defined above for slope stability analysis (Juang et al., 1992). They conducted several trial and error attempts with the parameters for the use in the study before establishing the network topology.

NEW PROPOSED APPROACH

Minimum inverse velocity method (MIV)

There have been many studies that have used the inverse velocity method for time of slope failure prediction analysis. The proposed method of using the MIV is a subtle but significant modification of the inverse velocity method. Most of the active mines have radar monitoring systems for geotechnical risk management analysis. The radar systems provide the deformation data of the area being scanned. The radar system is fitted with either a two-dimensional (2-D) or one- dimensional (1-D) scanning antenna. The system scans a region of the wall being monitored by transmitting a pulse and recording the phase of the return signal. While the system scans an area of the slope, it compares the reflected signal from each scan with the waveform from the previous scan in order to determine the amount of deformation that has taken place in the slope between the two scans (Chandarana et al., 2016). The radar data provide the opportunity to observe the pre-failure evolution from the initial small movements all the way up to failure. Three stages describe the pre-failure deformation process: primary, secondary and tertiary. These stages are like the ones observed in creep studies of geomaterials (Crosta and Agliardi, 2003; Federico et al., 2012; Saito 1996; Xu et al., 2011). The primary stage of the pre-failure evolution displays a decreasing strain rate, the secondary stage displays a constant strain rate, and the tertiary stage shows a rapidly increasing strain rate leading to failure (Figure 5). The primary, secondary and tertiary stages represent regressive, steady and progressive movements, respectively of a moving rock mass. When a displacement versus time graph displays the tertiary stage, it tends to infinity over a short time, indicative of a slope failure (Nie et al., 2016).

The main focus of analyzing slope stability is the progressive movement or the tertiary stage of the pre-failure evolution process, as these characteristics represent rapid change and a possible failure. A progressive displacement prompts the need for a closer look at the slopes. As the slopes move faster, it is important to make predictions of a possible slope failure time continuously. One of the commonly used methods is IV method. For IV method, the displacement over time data is used to calculate the velocity followed by the inverse velocity rate calculation. When the velocity and inverse velocity curves are plotted against time, it is evident that velocity follows the deformation curve and points towards infinity, whereas the inverse velocity curve approaches zero. The fact that the inverse velocity approaches zero provides the possibility to predict the time of slope failure at the point where the inverse velocity curve intersects the time axis.

In reality, there is conceivably no situation where a deformation would take place for ever. Hence, there is no possibility that the inverse velocity would reach exactly zero. The radar systems currently in use have a limitation on the range of movement that they can measure in each scan. The amount of deformation that can be measured in a single scan is roughly equal to half the wavelength of the radar signal (or its frequency). In other words, if the deformation taking place is larger than half the wavelength, the radar system will not be able to capture the entire movement, effectively causing a phase ambiguity. Due to this downside of all monitoring radar equipment, there is a limit on the maximum deformation measured in each scan. Therefore, we can calculate the maximum velocity that can be measured each day and

Figure 6. Demonstration of the use of minimum inverse velocity to analyze a failure 2 h before the failure at location X The blue line represents deformation; orange line represents inverse-velocity averaged over 60 min, the gray line represents inverse-velocity averaged over 1440 min. Dotted orange and gray lines represent the extended best fit lines of the data to help predict the time of failure. The red dotted line represents actual time of failure. The yellow horizontal line represents the minimum inverse velocity.

Table 1. IV vs. MIV failure time prediction for data in Figure 6.

Prediction	IV over 60	IV over 1440
IV Prediction	5/6/2014 2:41 AM	5/6/2014 4:41 AM
MIV Prediction	5/4/2014 8:23 PM	5/5/2014 4:38 AM

Scan time: 16 min; Failure time: 05/05/2014 5:04 AM; Minimum inverse velocity: 0.035773 day/in.

subsequently determine the minimum inverse velocity that is physically possible to obtain.

We now describe the process of calculating the MIV. We use the four steps described above to determine the inverse velocity, however, we also introduce an additional step that entails the determination of the minimum inverse velocity that the radar system would be able to measure in a given area being scanned. The minimum inverse velocity can be calculated as defined:

$$v = s * \frac{\left(C/R_f\right) * C_f}{4} \qquad (3)$$

$$v_{max} = v * 24 \qquad (4)$$

$$iv_{min} = 1/v_{max} \qquad (5)$$

Where: v = velocity (in/h); s = number of scans per hour; C = speed of light; R_f = radar frequency of the radar being used to monitor; C_f = conversion factor from m to in (required if readings are in inches) v_{max} = maximum velocity (in/day)

When the minimum inverse velocity is calculated it should be set as the y-value in the equation y = mx + b of the best fit line instead of using y=0.

The use of IV method had been successful in the past; however, often the predictions made fall in the unsafe zone, that is, the predicted time is located beyond the life expectancy of the slope or the actual failure time. A data set acquired from a mine site in

Arizona is used to illustrate the process: the visual aid will show the difference between the predictions in the safe and unsafe zone. Figure 6 illustrates the use of the MIV method, where a horizontal orange line is drawn to mark the location of the minimum inverse velocity. One can observe that the best fit line for the smoothed inverse velocity intersects the time axis past the red dotted line that represents the time of failure. However, the same best fit inverse velocity line intersects the minimum inverse velocity before the time of the failure, therefore providing a safe prediction.

While performing the analysis of data from a moving area, it is common practice to use a moving-average filter to smooth out the velocity (and inverse velocity) time series. This process reduces the high frequency noise which is the direct consequence of differentiating a time series. For the purposes of this paper, 60-min and 1440-min windows have been used for smoothing (Table 1).

The recorded time of failure at mine X was 5:04 AM on 5th May. To make a prediction, the best fit lines were used to calculate the time of failure with both the IV and MIV methods and using data from two hours before the failure. Using the inverse velocity averaged over 60 min, places the time of failure for the IV method at 6th of May 2:41 AM which is after the actual failure, whereas prediction for the MIV method is May 4th at 8:23 PM which is before the actual failure. Smoothing the velocity curve with a 1440-min window, yields a predicted time of 4:41 AM on May 6th which is after the actual failure, whereas the prediction for the MIV method is 4:38 AM on May 5th which places the forecast in the safe zone (prior to the actual time of failure). The results of the two methods are displayed in Table 1. The above example clearly demonstrates
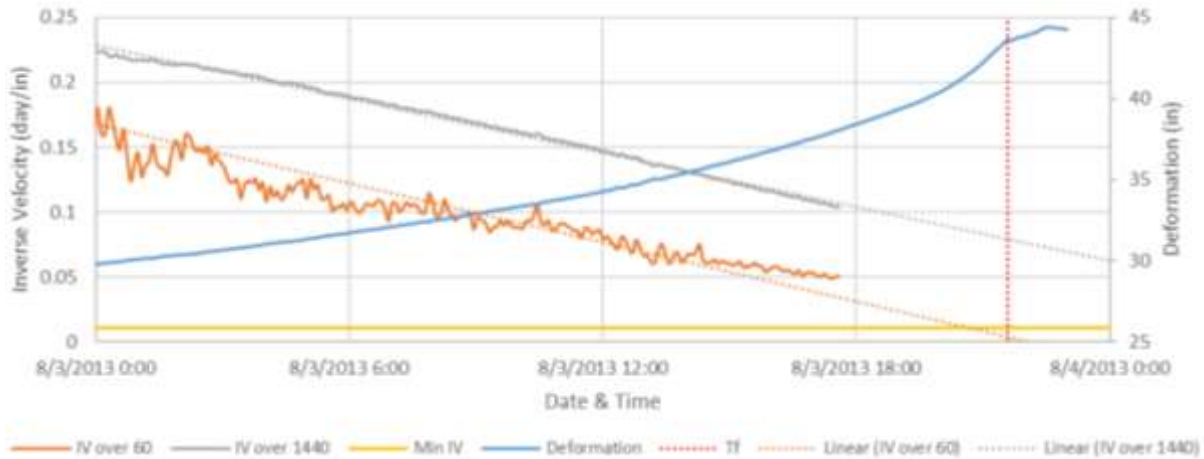
Figure 7. Demonstration of the use of minimum inverse velocity to analyze failure 4 h before the failure at location Y. The blue line represents deformation; orange line represents inverse-velocity averaged over 60 min, the gray line represents inverse-velocity averaged over 1440 min. Dotted orange and gray lines represent the extended best fit lines of the data to help predict the time of failure. The red dotted line represents actual time of failure. The yellow horizontal line represents the minimum inverse velocity.

Table 2. IV vs. MIV failure time prediction for data in Figure 7.

Prediction	IV over 60	IV over 1440
IV Prediction	8/3/2013 10:16 PM	8/4/2013 8:46 PM
MIV Prediction	8/3/2013 8:47 PM	8/4/2013 6:20 PM

Scan time: 5 min; Failure time: 08/03/2013 10:06 PM; Minimum inverse velocity: 0.011179 days/in.

that using the MIV method has the potential to turn an unsafe prediction into a safe prediction. The prediction times for the IV method might be closer to the actual time of failure; however, a disadvantage of the method is that it provides a prediction time that is past the failure leaving no room to remove employees and equipment from any hazardous areas.

In another case study related to the application of the MIV method, we show the data collected from site Y (Figure 7 and Table 2). In this case, the recorded failure time was 10:06 PM on 3rd August, 2013 with a scan period of 5 min per scan and a calculated minimum inverse velocity of 0.011179 day/in. While analyzing the inverse velocity data averaged over 60 min, the IV method gave a prediction of 10:16 PM on 3rd August, 2013 whereas the MIV method gave a prediction of 8:47 PM on 3rd August 2013. For this site, the IV method's forecast falls in the unsafe zone, while the MIV method provides a safe prediction. When the same dataset is analyzed using a moving-average window of 1440 min, the prediction with the IV method yields a value of 8:46 PM on 4th August 2013, and 6:20 PM on 4th August 2013 with MIV method. With the 1440-min window, neither method provides a safe prediction; however, the MIV method is closer to the actual time of failure.

Maximum velocity method (MV)

No evidence has been found in the literature for velocity being used to predict the time of slope failure. An attempt has been made in this paper to demonstrate that velocity can be used to get an estimate of the time of slope failure similar to the use of inverse velocity. Similar to the MIV method, the MV method uses the frequency of the radar, the wavelength and the time per scan to calculate the maximum velocity.

It is noteworthy to reiterate that the IV method has become popular because of the fact that the inverse velocity of an accelerating slope approaches zero. However, the tendency of the velocity curve to follow the shape of the deformation curve and approach infinity makes it difficult to get a close fit straight line to the data and obtain a reliable prediction.

The effort to use velocity for predicting the time of failure follows the use of minimum inverse velocity. We mentioned previously that radar systems have a limit on the range of deformation they can measure during a given scan. The maximum deformation that can be obtained in a day, from a radar scan is calculated based on the maximum allowance of measurement per scan. In most cases, the radar readings will approach the maximum velocity only if the slope is moving too fast where the fast-moving slope is indicative of a possible failure. It is however assumed that the time it takes for the radar to reach the maximum velocity/day, will be the same as the predicted failure time. An attempt was therefore made to use this approach to forecast failure times. Based on our analysis, about 45% of the predictions were either in the safe zone or closer to the actual failure time.

The use of MV method was inspired by the question: If inverse velocity that is generated from velocity can be used to predict time of failure then why can velocity not be used in a similar manner to predict the time of failure? The problem encountered while using the velocity curve to make predictions was the shape of the curve.

Figure 8. Demonstration of the use of maximum velocity for slope failure prediction at location A. The blue line represents deformation; yellow line represents velocity averaged over 60 min. The green dotted line represents the extended SPLINE to help predict the time of failure. The red dotted line represents actual time of failure. The orange horizontal line represents the maximum velocity.

Any attempt to fit a straight best-fit line through the velocity curve would not give a reliable prediction. To overcome this problem, the Bessel SLINE was used to fit through the velocity curve in order to make predictions using velocity data.

When attempting to use the velocity curve of a moving slope, it is advisable to use the data past the inflection point – the point of maximum curvature – in the deformation curve. The shape of the velocity curve does not allow close fit of a straight line in order to make a reliable prediction. For the purposes of this study, a Bessel SPLINE curve was fit through the velocity curve and extended to intersect the maximum velocity (in/day) line as shown in Figure 8. The maximum velocity is different for each dataset since the scan time for each area would be different. The five simple steps below define the use of MV method:

1) Find the Maximum Velocity (in/day) for your data set using the v_{max} equation demonstrated previously.
2) Narrow down the data set to include the data demonstrating the progressive trend of moving slope. Discard all the data points prior to the visible progressive trend in the data.
3) Create a new set of time values that include the minimum and maximum time of the dataset, while keeping the time interval between the new time values less than half the scan time. It is important to have time values that go past the last available time data point.
4) Use the SPLINE function to generate new velocity values based on the new time values. The SPLINE function helps populate new deformation value for the new time values based on the original data. The function helps fill in the holes to generate the best-fit line of a curve that can be extended to follow the initial curvature of the line.
5) Graph the SPLINE values, find the intersecting point of the extended velocity curve and the maximum velocity. The intersecting point between the velocity curve and the maximum velocity will be the failure time prediction.

Figures 8 and 9 provide an illustration of the use of maximum velocities for two different failures. Figure 8 shows the use of the MV method for site A. In this case, the calculated v_{max} is 49.7 in/day, the real time of failure 4:17 PM on 25th October 2012 and the prediction from the extended SPLINE is 4:21 PM on 25th October, 2012, which is approximately within 5 min of the actual

failure time. This prediction is very close to the real time of failure. Figure 9 shows another example of using the MV method. The calculated v_{max} is 40.7 in/day, the real time of failure 10:24 PM on 20th June 2009 and the failure prediction 12:36 AM on 21st June 2009, making this prediction approximately 2 h past the actual time of failure. The application of the MV method to 22 datasets at our disposal provided 45% better predictions compared to the popular IV method.

RESULTS

In order to analyze and compare the performance of the proposed minimum inverse velocity method with the IV method, 22 datasets from seven different surface mines were analyzed. Table 3 summarizes the results of the analysis. The time difference between the actual time of failure and IV ranged from approximately -0.48 to 362 h, whereas the time difference between the real time of failure and MIV ranged from ~ -8.67 to 2.92 h. The data in Table 3 shows predictions based on the IV and MIV methods for each failure analyzed. It also shows the difference between the two methods for each slope failure. The column "IV – MIV" provides the time difference between the two approaches. Positive values represent the number of hours MIV prediction is closer to the real time of failure compared to IV. Each positive value in the "IV – MIV" column represents a success for MIV, while each negative value represents a success for IV. Based on the results presented above 16 of the 22 failures analyzed gave a better result using MIV method. In the 16 cases that demonstrate a better prediction, the smallest improvement is about 0.05 hours while the largest improvement is 360 h. The success rate for the MIV results in a 75% improvement in slope failure predictions compared to the IV method.

Figure 9. Demonstration of the use of maximum velocity for slope failure prediction at location B. The blue line represents deformation; yellow line represents velocity averaged over 60 minutes. The green dotted line represents the extended SPLINE to help predict the time of failure. The red dotted line represents actual time of failure. The orange horizontal line represents the maximum velocity.

Table 3. Comparison between Inverse Velocity Method (IV) and Minimum Inverse Velocity Method (MIV) from 22 different failure examples.

S/N	Actual time of failure	Prediction: IV	Delta time (h)	Prediction: MIV	Delta time (h)	IV – MIV (h)
1	3/2/14 4:23	3/2/14 5:55	1.54	3/2/14 5:48	1.42	0.12
2	10/25/12 16:17	10/25/12 16:47	0.51	10/25/12 15:35	-0.69	-0.18
3	4/22/13 13:27	4/22/13 13:58	0.52	4/22/13 10:02	-3.40	-2.88
4	3/14/10 4:01	3/14/10 4:16	0.26	3/14/10 4:02	0.03	0.24
5	7/11/13 0:20	7/11/13 0:25	0.10	7/11/13 0:13	-0.11	-0.01
6	7/21/11 15:01	7/21/11 15:17	0.28	7/21/11 14:35	-0.42	-0.14
7	3/10/09 7:12	3/10/09 7:51	0.65	3/10/09 7:42	0.52	0.13
8	6/20/09 22:24	6/21/09 1:09	2.76	6/20/09 23:58	1.57	1.20
9	2/9/10 12:38	2/9/10 14:05	1.47	2/9/10 13:20	0.71	0.75
10	1/30/15 18:25	1/30/15 21:55	3.51	1/30/15 21:11	2.78	0.74
11	5/5/14 5:04	5/6/14 2:41	21.62	5/4/14 20:23	-8.67	12.96
12	6/16/14 6:58	6/16/14 7:10	0.21	6/16/14 4:01	-2.95	-2.74
13	1/28/12 9:14	1/28/12 12:04	2.84	1/28/12 9:08	-0.10	2.74
14	10/29/12 12:15	10/31/12 18:58	54.73	10/29/12 11:58	-0.28	54.45
15	9/25/12 8:40	9/26/12 18:16	33.61	9/25/12 4:33	-4.12	29.49
16	3/26/13 21:03	4/10/13 23:08	362.10	3/26/13 23:58	2.92	359.18
17	2/24/12 11:27	2/24/12 17:03	5.61	2/24/12 13:42	2.26	3.36
18	3/13/13 9:48	3/13/13 9:19	-0.48	3/13/13 8:45	-1.04	0.56
19	3/5/12 4:09	3/5/12 4:34	0.43	3/5/12 4:31	0.38	0.05
20	8/3/13 22:06	8/3/13 23:53	1.79	8/3/13 22:15	0.16	1.63
21	7/27/12 18:50	7/27/12 19:38	0.81	7/27/12 19:00	0.18	0.64
22	10/24/13 22:39	10/24/13 22:40	0.03	10/24/13 20:58	-1.68	-1.65

For the analysis demonstrated, all calculations are based on a 60-min averaging window.

A 95% confidence interval was calculated for both methods. The results are shown in Table 4. Based on the confidence interval calculations we can conclude that 95% of the slope failure predictions calculated using the

Table 4. Confidence interval calculated for the IV and MIV methods.

Statistical parameter	95.5% Confidence interval	
	IV Method	**MIV Method**
Mean (μ)	22.5	-0.48
Standard deviation (σ)	77.04	2.57
Upper limit	176.52	4.66
Lower limit	-131.39	-5.62

The calculations use μ±2σ to get the upper and lower bounds of the 95.5% confidence interval.
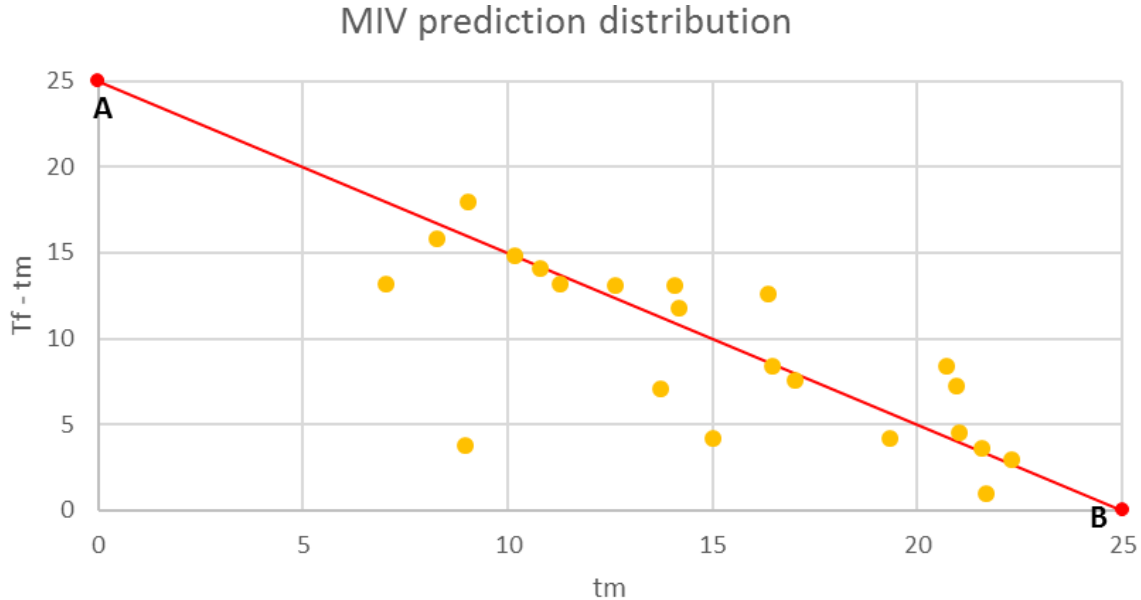
IV prediction distribution
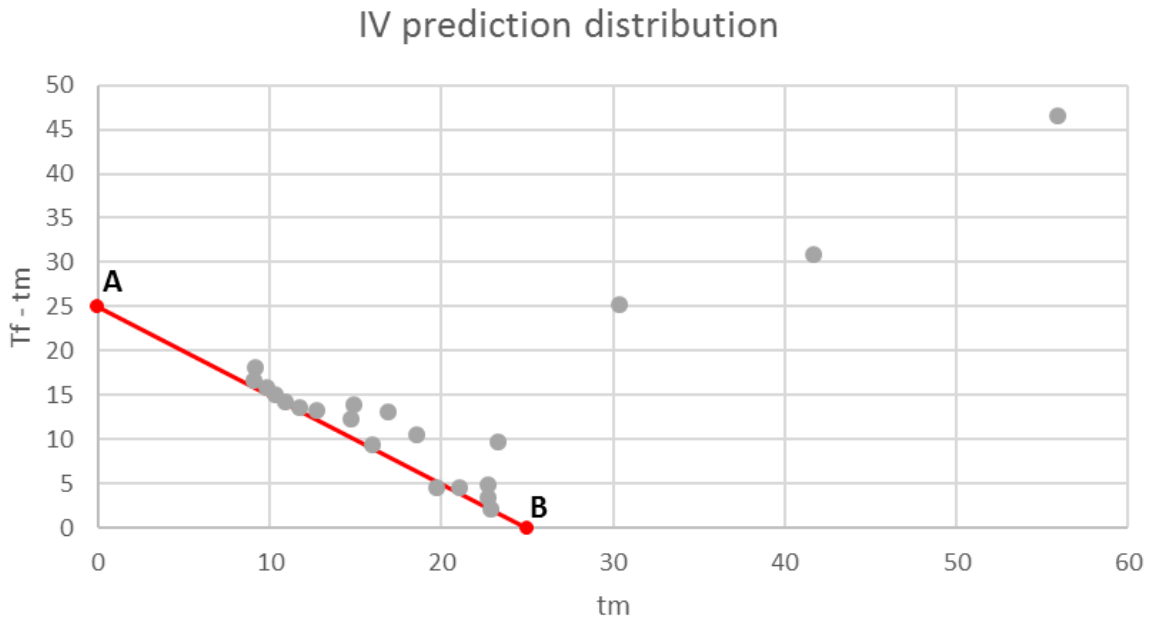
Figure 10. Distribution of failure predictions using IV method. Line AB represents failure time.

IV method will fall between -131 and 176 h away from the real time of failure. When the confidence interval was applied to the datasets used for analysis, 21 of the predictions fell in the 95% CI using IV method. The prediction as well as get a safe failure prediction. The time difference between the real time of failure and predictions made using IV and MIV method were rotated 45° and plotted on an x-y plot in Figures 10 and 11 to represent the safe vs. unsafe prediction visualization similar to Figure 2. While Table 3 shows all the failure predictions using IV and MIV method, Figure 10 demonstrates the distribution of failure predictions using the IV method in relation to the time of failure. The outlier with a time difference of 362 h in the data set from IV predictions was eliminated from the graph to demonstrate a better visualization of the rest of the data. From the distribution of IV predictions, it is visible that some failure predictions are close to the actual time of failure, but only one prediction is before the failure. Figure 11 demonstrated the distribution of failure predictions using

confidence interval calculated for MIV indicate that 95% of the slope failure predictions calculated using MIV will fall between -6 and 5 h away from the real time of failure. Twenty-one of the 22 data sets analyzed gave a time of MIV method about the time of failure. Any point in Figure 11 below the red line represents a failure prediction before the actual failure time and corresponds to a negative value in Table 3. Based on the data demonstrated in Figure 11 it is evident that 50% of the failures have a prediction in the safe zone. The comparison between failure predictions using IV and MIV shows an improvement in time of failure predictions when MIV method is used.

DISCUSSION

Risk management analysis is crucial as there is always room for unanticipated ground movement on the surface or underground. The unexpected movement leads to

Figure 11. Distribution of failure predictions using MIV method. Line AB represents failure time.

hazardous conditions that could endanger lives and demolish expensive equipment. Several measures can be taken to help reduce the effects of ground failure including the use of monitoring devices to provide advance warning, safe geotechnical design, secondary supports or rock catchment systems, etc. (Girard and McHugh 2000).

In the mining industry and the topic at hand, it is clear that failure prediction is a crucial part of all geomechanical analysis. The use of a displacement versus time plot is the first common step for any failure analysis. When the displacement trend enters the tertiary stage, it tends to increase asymptotically towards failure. As the initial signs of failure are visible from monitoring data it is important to analyze the data and make some failure predictions to ensure the safety of the employees and company assets. For the research purpose of this paper, many different variations of analysis were used. Similar to any experiment there were a few successful and unsuccessful results for the analysis of time failure prediction of an unstable area in an active mine site. The successful methods used for the purpose of this paper included the MIV and the MV methods as described above.

Many researchers have concluded that the inverse velocity method as defined by Fukuzono (Mufundirwa et al., 2010) is a very powerful tool for making slope failure predictions and has been used for failure analysis to date. This method has been highly popular through the decades and has provided close to real time predictions of failures. Many of these predictions fall into the unsafe zone despite being close to the actual time of failure. For the time of slope failure analysis, inverse velocity and velocity trends are assumed to be linear and approaching zero or infinity, for predicting the time of failure. The linearity assumption is heavily dependent on any instrumental and natural noise in the data (Carlá et al., 2017b). As noise is present in any data due to natural or unnatural conditions, data smoothing is a crucial part of slope stability analysis. Usually, the data is smoothed over 60 min or over 24 h. The smoothing over 60 and 1440 min is used as the minimum and maximum values for the failure prediction window. The smoothing over 1440 can be changed based on the requirements of each mine site. The smoothing over 60 min allows the data to be close to the actual reading and not removing all the noise found in the data. Whereas smoothing over 1440 min permits the removal of most noise and makes the data very smooth.

Successes

Minumum inverse velocity method

This paper presents an improvement to the existing inverse velocity method for predicting the time of slope failure by shifting the predicted time of failure into the safe zone. The enhancement incorporates the use of minimum inverse velocity in the calculation of the time of failure. The minimum inverse velocity is calculated based on the wavelength of the radar used and the number of scans per hour. As mentioned above, data smoothing is an important step in the process to reduce the amount of high-frequency noise introduced after taking the derivative of the deformation data. For all the case

studies in this paper, the data was smoothed using a 60-min window. Figures 6 and 7 visually exhibit that the use of the MIV method helps convert unsafe predictions into safe predictions. One advantage of using the minimum inverse velocity is that the limitations of the radar systems are taken into consideration, allowing for the majority of predicted failure times to occur before the actual failure and prolonging the life expectancy curve for the moving area.

Two different smoothing time intervals were chosen to calculate a time prediction window with an upper and lower limit between which the failure might occur. The data smoothed over 60 min provides the lower limit of the time window and the smoothing over 1440 min contributes the upper bound of the failure prediction window. There could be a few rare cases where the situation might be reversed; however, none of the data analyzed in this paper showed that trend. The primary purpose of this study was to show an improvement in the time of failure prediction using the new proposed MIV method. Table 3 illustrates a detailed comparison between the IV and MIV methods. For the purpose of the analysis carried out in this investigation, the inverse velocity was smoothed over a 60-min period. The results in Table 3 show a 75% improvement in the slope failure predictions made using the MIV method.

Maximum velocity method

Application of the maximum velocity method is similar to the MIV method. When calculating the time of failure, we rely on the fact that the deformation and velocity trends get steeper and more linear as we get closer to the actual time of failure. To use the MV method, the first step is to calculate the maximum velocity the radar can measure in a day based on the wavelength and the time it takes to complete one scan. Once an accelerating trend is observed in the deformation curve, analysis can be started. In the case studies presented above, a Bessel SPLINE function was fit to the velocity curve shortly past the inflection point (the point of maximum curvature) in the deformation curve. The extended SPLINE line was then used to find the intersection point on the maximum velocity line. The predicted time of failure was then obtained at the intersection point. This method was successful in getting close predictions to the actual time of failure, however, only about half the predictions fell in the safe zone.

When using radar data, it is important to remember that the data captured by the radar is influenced by the line-of-sight (LOS) between the sensor and the area of interest. The recorded displacement of the slope movement could be considerably lower than the actual total displacement based on the setup of the radar and the angle at which the deformation is measured (Carlá et al., 2017a). If the LOS does not allow the radar to capture the true deformation, the calculated velocity will be lower, hence further away from the maximum velocity range of the radar resulting in predictions further away from the real time of failure. A potential disadvantage of this method is the effect of smoothing on the predicted values. Smoothing the data using a window longer than 60 min tends to push the prediction times further out into the future (past the actual failure time). The projections are pushed out into the unsafe zone because the velocity curve loses its steepness with higher smoothing denominations. The data will always be noisy close to the actual failure and oversmoothing the velocity might reduce the influence of the data points prior to failure. Since this technique provided reliable predictions less than 50% of the time, the authors hope that this approach could potentially be improved with the help of machine learning techniques.

Challenges

Use of log inverse velocity (IV) and log velocity (V) curve

As previously mentioned, there are three types of slope movement encountered at a mine site: progressive, regressive and steady movement. Progressive movement is the primary concern when it comes to unstable slopes. In 1985 when Fukuzono established the inverse velocity method for slope failure predictions, he performed tests to identify if a concave, convex or linear trend line would provide the most accurate time of failure. He concluded that a linear fit gives the best predictions (Fukuzono, 1985). Since the inverse velocity method was established, linear trend lines have been fit through the inverse velocity curves to make predictions. When looking at a real data set, it is clear that a velocity curve follows the shape of the deformation curve, so it would seem inappropriate to fit a straight line to data that exhibit an exponential trend.

It is a well-known fact that the use of the logarithm function can help linearize an exponential curve; therefore an attempt was made to use the log of IV values for the analysis of data. Converting the IV into log values provided an almost linear trend; however, it made the slope of curve much steeper. Extending the best fit line of the log of IV values intersected the x-axis much earlier than the actual failure time, making the failure prediction extremely inaccurate. The intent to use the log values was to bring the failure time prediction closer to the actual failure time, however, the analysis of the data had the opposite effect. The use of this method for time of failure prediction was not as successful as anticipated. Along with the log of IV, an attempt was made to use the log of the velocity curve to intersect the maximum velocity line. Similar to the log of the inverse velocity values this method did not produce the intended results. In this case

also, the log values helped linearize an exponential-looking curve, however, using log function made the slope much shallower. This has the net effect of pushing the predictions deeper into the unsafe zone and increasing the gap between the actual and the predicted time of failure.

Conclusion

The ultimate objective of a geotechnical risk management analysis is to successfully manage slope instabilities that pose a threat to personnel, equipment and continued production of the mine (Chandarana et al., 2016). Unforeseen slope movements have occurred in the past and continue to be an issue today regardless of all the precautions taken during the initial phases of mine design (Harries et al., 2006). Geotechnical risk management analysis is used to reduce the danger of unforeseen slope failures. The primary reason for accurate slope failure prediction is to provide sufficient time to evacuate workers and machinery from the affected areas safely. Based on the different methods of analysis evaluated in this paper, the minimum inverse velocity method outperformed the existing and popular inverse velocity method in all the cases. More studies are required to further evaluate the performance of the MIV method for the purpose of slope failure analysis. Finally, slope failures can be estimated but cannot be fully controlled. While different data analysis techniques are being developed to improve prediction times, a phenomenological model taking into account all the factors affecting instability may provide the best option to obtain estimates of slope failure.

CONFLICT OF INTERESTS

The authors have not declared any conflict of interests.

REFERENCES

Cahill J, Lee M (2006). Ground control at Leinster Nickel Operations. In Proceedings on the International Symposium of Rock Slopes in Open Pit Mining and Civil Engineering. The South African Institute of Mining and Metallurgy. pp. 321-334. https://www.saimm.co.za/Journal/v106n07p471.pdf

Call RD, Cichini PF, Ryan TM, Barkley RC (2000). *Managing and analyzing Overall Pit Slopes.* In: Hustrulid WA, McCarter MK, Van Zyl DJA, Slope Stability in Surface Mining. pp. 39-46.

Carlá T, Intrieri E, Farina P, Casagli N (2017a). A new method to identify impending failure in rock slopes. Int. J. Rock Mech. Min. Sci. 93:76-81.

Carlá T, Intrieri E, Traglia FD, Nolesini T, Gigli G, Casagli N (2017b). Guidelines on the use of inverse velocity method as a tool for setting alarm thresholds and forecasting landslides and structure collapses. Landslides. 14(2):517-534. https://doi.org/10.1007/s10346-016-0731-5.

Chandarana UP, Momayez M, Taylor K (2016). Monitoring and predicting slope instability: a review of current practices from a mining perspective. Int. J. Res. Eng. Technol. 5(11):139-151.

https://doi.org/10.15623/ijret.2016.0511026

Chen H, Zeng Z, Tang H (2015). Landslide deformation prediction based on the recurrent neural network. Neural Process. Lett. 41(2):169-178. https://doi.org/10.1007/s11063-013-9318-5.

Crosta GB, Agliardi F (2003). Failure forecast for large rock slides by surface displacement measurements. Can. Geotechnical J. 40:176-191. https://doi.org/10.1139/t02-085

Day AP, Seery JM (2007). Monitoring of a large wall failure at Tom Price iron ore mine. In: Proceedings of the International Symposium on Rock Slope Stability in Open Pit Mining and Civil Engineering. Australian Center of Geomechanics. pp. 333-340.

Dick GJ, Eberhardt E, Cabrejo-Lievana AG, Stead D, Rose ND (2015). Development of an early-warning time-of-failure analysis methodology for open-pit mine slopes utilizing ground-based slope stability radar monitoring data. Can. Geotechnical J. 52 (4):515-529. https://doi.org/10.1139/cgj-2014-0028

Federico A, Popescu M, Fidelibus C, Interno G, Murianni A (2012). Prediction of time to slope failure a general framework. Environ. Earth Sci. 66(1):245-256. https://doi.org/10.1007/s12665-011-1231-5

Fukuzono T (1985). A new method for predicting the failure time of a slope. IN: Proceedings of the fourth international conference and field workshop on landslides. Tokyo, Japan Landslide Society. pp. 140-150.

Girard JM, McHugh E (2000). Detecting problems with mine slope stability. In: 31st Annual Institute on Mining Health, Safety, and Research, Roanoke, VA. NIOSHTIC 2:1-8. https://www.cdc.gov/niosh/mining/works/coversheet1303.html

Harries NJ, Roberts H (2007). The use of Slope Stability Radar (SSR) in managing slope instability. In Rock Mechanics: Meeting Society's Challenges and Demands, Proceedings of the 1st Canada-US Rock Mechanics Symposium: 53-60. https://doi.org/10.1201/NOE0415444019-c7

Harries N, Noon D, Rowley K (2006). *Case studies of slope stability radar used in open cut mines.* Proceedings of Stability of Rock Slopes in Open Pit Mining and Civil Engineering Situations, Cape Town, South Africa. pp. 335-342. http://www.sujyoti.com/wp-content/themes/sujyoti/pdf/Slope-Stability-Radar.pdf

Hwang S, Guevarra IF, Yu B (2009). Slope failure prediction using a decision tree: A case of engineered slopes in South Korea. Eng. Geol. 104:126-134. https://doi.org/10.1016/j.enggeo.2008.09.004

Intrieri E, Gigli G, Mugnai F, Fanti R, Casagli N (2012). Design and implementation of a landslide early warning system. Eng. Geol. 147(148):124-136. https://dx.doi.org/10.1016/j.enggeo.2012.07.017

Juang CH, Lee DH, Sheu C (1992). *Mapping slope failure potential using fuzzy sets.* J. Geotechnical Eng. ASCE. 118(3):475-494. http://dx.doi.org/10.1061/(ASCE)0733-9410(1992)118:3(475)#sthash.dVrsWmrU.dpuf

Lin HM, Chang SK, Wu JH, Juang CH (2009). Neural network-based model for assessing failure potential of highway slopes in the Alishan, Taiwan area: pre- and post- earthquake investigation. Engineering and Geology 104:280-289. https://doi.org/10.1016/j.enggeo.2008.11.007

Little MJ (2006). Slope monitoring at PPRust open pit operation. In Proceedings of the International Symposium on Stability of Rock Slopes in Open Pit Mining and Civil Engineering. The South African Institute of Mining. pp. 211-230. http://www.saimm.co.za/Conferences/RockSlopes/211-230_Little.pdf

Liu Z, Shao J, Xu W (2014). Comparison on landslide nonlinear displacement analysis and prediction with computational intelligence approaches. Landslides 11(5):889-896. https://doi.org/10.1007/s10346-013-0443-z

Mazzanti P, Bozzano F, Cipriani I (2015). New insights into the temporal prediction of landslides by a terrestrial SAR interferometry monitoring case study. Landslides 12(1):55-68. https://doi.org/10.1007/s10346-014-0469-x.

Mufundirwa A, Fujii Y, Kodama J (2010). A new practical method for prediction of geomechanical failure-time. Int. J. Rock Mech. Min. Sci. 47:1079-1090. https://doi.org/10.1016/j.ijrmms.2010.07.001.

Ni SH, Lu PC, Juang CH (1996). Fuzzy neural network approach to evaluation of slope failure potential. Microcomput. Civil Eng. 11:56-66. https://doi.org/10.1111/j.1467-8667.1996.tb00309.x

Nie L, Li Z, Lv Y, Wang H (2016). A new prediction model for rock slope

failure time: a case study in West Open-Pit Mine, Fushun, China. In: Bulletin of Engineering Geology and the Environment. pp. 1-14. https://doi.org/10.1007/s10064-016-0900-8

Osasan KS, Stacey TR (2014). Automatic prediction of time to failure of open pit mine slopes based on radar monitoring and inverse velocity method. Int. J. Min. Sci. Technol. 24(2):275-280. https://doi.org/10.1016/j.ijmst.2014.01.021.

Ozbay A, Cabalar AF (2014). FEM and LEM stability analyses of the fatal landslides at Çöllolar open-cast lignite mine in Elbistan, Turkey. Landslides 12:155-163. https://doi.org/10.1007/s10346-014-0537-2

Ramsden F, Coli N, Benedeitt AI, Falomi A, Leoni L, Michelini A (2015).

Effective use of slope monitoring radar to predict a slope failure at Jwaneng Mine, Botswana. The Southern African Institute of Mining and Metallurgy. Slope Stability. https://www.idscorporation.com/images/Downloads/GeoRadar/IBIS_White_Papers/Effective_use_of_slope_monitoring_radar_to_predict_a_slope_failure_at_Jwaneng_Mine_Botswana.pdf

Rose ND, Hungr O (2006). Forecasting potential rock slope failure in open pit mines using inverse-velocity method. Int. J. Rock Mech. Min. Sci. 44(2):308-320. https://doi.org/10.1016/j.ijrmms.2006.07.014.

Saito M (1996). Forecasting time of slope failure by tertiary creep. In: Proceedings of the 7th International Conference on Soil Mechanics and Foundation Engineering. pp. 677-683. http://citeseerx.ist.psu.edu/viewdoc/download?doi=10.1.1.612.2877a ndrep=rep1andtype=pdf.

.

Sakellariou MG, Frentinou MD (2005). A Study of slope stability prediction using neural networks. Geotechnical Geological Eng. 23:419- 425. https://doi.org/10.1007/s10706-004-8680-5

Wang HB, Xu WY, Xu RC (2005). Slope Stability evaluation using propagation neural networks. Eng. Geol. 80:302-315. https://doi.org/10.1016/j.enggeo.2005.06.005

Xu Q, Yuan Y, Zeng YP (2011). Some new pre-warning criteria for creep slope failure. Sci. China Technological Sci. 54(1):210-220. https://doi.org/10.1007/s11431-011-4640-5.

Zadeh LA (1965). *Fuzzy sets*. Information and control 8(3):338-353. https://doi.org/10.1016/S0019-9958(65)90241-X

Zavodni ZM, Broadbent CD (1978). Slope Failure Kinematics. Preprint Proceedings 19th US Symposium on Rock Mechanics 2:86-94. https://www.onepetro.org/conference-paper/ARMA-78-0102.